HGT

Prenatal Intraportal Delivery of Polymeric Nanoparticles to Fetal Rhesus Monkeys (*Macaca mulatta*)

Alexandra S. Piotrowski-Daspit,[1–3,†] Anna Y. Lynn,[3,†] David A. Eaton,[3] Laura G. Bracaglia,[4] Arianna I. Markey,[1] Ryland D. Mortlock,[3] David H. Stitelman,[5] Michele L. Martinez,[6,7] Charles C. Lee,[7,8] Harvey J. Kliman,[9] Peter M. Glazer,[10,11,‡] Alice F. Tarantal,[6–8,‡,*] and W. Mark Saltzman[3,12–14,*,‡]

[1]*Department of Biomedical Engineering, University of Michigan, Ann Arbor, Michigan, USA;* [2]*Department of Internal Medicine – Pulmonary & Critical Care Medicine Division, University of Michigan, Ann Arbor, Michigan, USA;* [3]*Department of Biomedical Engineering, Yale University, New Haven, Connecticut, USA;* [4]*Department of Chemical & Biological Engineering, Villanova University, Villanova, Pennsylvania, USA;* [5]*Department of Surgery, Yale University, New Haven, Connecticut, USA;* [6]*Department of Pediatrics, University of California, Davis, California, USA;* [7]*California National Primate Research Center, University of California, Davis, California, USA;* [8]*Department of Cell Biology and Human Anatomy, School of Medicine, University of California, Davis, California, USA;* [9]*Department of Obstetrics, Gynecology & Reproductive Sciences, Yale University, New Haven, Connecticut, USA;* [10]*Department of Therapeutic Radiology, Yale University, New Haven, Connecticut, USA;* [11]*Department of Genetics, Yale University, New Haven, Connecticut, USA;* [12]*Department of Chemical & Environmental Engineering, Yale University, New Haven, Connecticut, USA;* [13]*Department of Cellular & Molecular Physiology, Yale University, New Haven, Connecticut, USA; and* [14]*Department of Dermatology, Yale School of Medicine, Yale University, New Haven, Connecticut, USA.*

[†]*Co-first authors.*

[‡]*Co-senior authors.*

Preliminary investigations focused on biodistribution of polymeric nanoparticles (NPs) shortly after ultrasound-guided delivery via the portal vein in early second-trimester fetal rhesus monkeys. Results demonstrated that poly(lactic-co-glycolic acid) (PLGA) NPs (N = 3; 3 mg administered at 75–80 days gestational age) and poly(amine-co-ester)-polyethylene glycol (PACE-PEG) NPs (N = 3; 3 mg at 75–80 days gestational age) distributed to fetal tissues when assessed 24 h post-administration. No adverse findings were observed. PLGA NPs were found primarily in the fetal liver and spleen, whereas PACE-PEG NPs showed more widespread biodistribution to a range of anatomical sites. In another fetal subset with PACE-PEG NPs (N = 2; 90 days gestational age) assessed within 48-h post-administration, results demonstrated enhanced green fluorescent protein reporter mRNA expression in select tissues. These early-stage short-term studies suggest that polymeric NPs, particularly those composed of PACE-PEG, can be safely administered and are potential candidates for fetal delivery of therapeutic nucleic acids. While preliminary, these studies provide evidence to support further investigations in this species to address long-term safety and efficiency.

Keywords: nanoparticles, fetal rhesus macaque, intraportal delivery, biodistribution

INTRODUCTION

Nanoparticles (NPs) composed of biodegradable and biocompatible polymers are highly tunable delivery vehicles that can be optimized for efficient cargo encapsulation, extended time in circulation, and controlled release. One commonly used polymer is poly(lactic-co-glycolic acid) (PLGA), which is commercially available, biodegradable, non-toxic, and has been applied successfully for gene editing and other therapeutic nucleic acid applications.[1–5] PLGA has also been assessed in biomedical devices, including drug delivery systems that have been approved by the U.S. Food and Drug Administration (FDA). However, when formulating NPs, it is important to consider the dynamic interplay between the NP material and the cargo and the resultant effects on encapsulation efficiency. Although PLGA NPs can be used for delivery of nucleic acids, they are inefficient in comparison to cationic polymers.[6]

Despite the greater efficiency of cationic polymers such as poly(ethylenimine) and poly(β-amino esters), these polymers have been shown to not be well tolerated *in vivo*.[7–9] Poly(amine-co-esters) (PACEs) are customized polymers in which the cation density can be reduced by the incorporation of hydrophobic groups. These polymers have been shown to provide high encapsulation efficiency of nucleic acids, as well as high cellular association and

*Correspondence: Dr. W. Mark Saltzman, Department of Biomedical Engineering, Yale University, Malone Engineering Center 413, 55 Prospect Street, New Haven, Connecticut, USA. E-mail: mark.saltzman@yale.edu; Dr. Alice F. Tarantal, Department of Pediatrics, University of California, One Shields Avenue, Davis, California, USA. E-mail: aftarantal@ucdavis.edu

DOI: 10.1177/10430342251414881

tolerability *in vitro* and *in vivo*.[10–14] Poly(ethylene glycol) (PEG), another polymer that is in a range of FDA-approved products, is often used as a surface modification for NPs because it serves as a stealth moiety by shielding NPs from serum protein adsorption as well as detection by phagocytic cells in the mononuclear phagocytic system.[15–17] However, there are questions about the consequences of anti-PEG immune responses, and thus this material requires careful consideration when used.[18] The biodistribution and transfection capabilities of PACE can be modulated and potentially enhanced by formulating NPs using a PACE-PEG block co-polymer.[12,13,19] The ability to modify the characteristics of the materials chosen for NP formulations, including core polymer and surface modifications, offers the opportunity to hone the *in vivo* behavior and delivery profile of these vehicles for a range of applications, including gene editing.[20]

In selecting a model for translational assessments of NPs for future clinical applications, it is essential to consider the developmental, anatomical, and physiological similarities when comparing the model species and humans. Nonhuman primates, particularly rhesus macaques, are ideal models for the study of human development and disease based on similarities in placentation, organ ontogeny, physiology, immunology, and genetics.[21] In this early-stage preliminary short-term study, the biodistribution of PLGA and PACE-PEG NPs was investigated 24 h after fetal intraportal administration in the early second trimester. Additionally, a short time frame study (48 h) allowed for the assessment of PACE-PEG NPs to deliver enhanced green fluorescent protein (EGFP) reporter mRNA in a subset of fetuses. These studies showed the safe and successful transfer of polymeric NPs using an established intraportal ultrasound-guided approach,[22] with no adverse effects detected during the study period. These studies support further investigations with polymeric NPs, particularly those composed of PACE-PEG, as potential candidates for fetal delivery of therapeutic nucleic acids that may be considered in the future for the treatment of a range of inherited disorders.

MATERIALS AND METHODS

Reagents

Poly(D,L-lactide-co-glycolide) (50:50 LA:GA, inherent viscosity: 0.55 to 0.75 dL/g) was purchased from Lactel and used as received. Acetonitrile and dimethyl sulfoxide (DMSO) were purchased from J.T. Baker (Philipsburg, NJ). Poly(vinyl alcohol) (PVA) was purchased from Sigma-Aldrich (St. Louis, MO). 15-pentadecalactone (PDL, 98%), diethyl sebacate (DES, 98%), sebacic acid (SA, 98%), N-methyldiethanolamine (MDEA, 99+%), polyethylene glycol (PEG, 5000 MW), diphenyl ether (99%), immobilized *Candida antarctica* lipase B (CALB) supported on Novozym 435, chloroform (HPLC grade), chloroform-*d* (NMR grade), dichloromethane (HPLC grade, 99+%), hexanes (HPLC grade, 97+%), and methanol (98%) were all purchased from Sigma Aldrich and used as received. 1,1'-dioctadecyl-3,3,3′,3′-tetramethylindodicarbocyanine, 4-chlorobenzenesulfonate salt (DiD) dye was obtained from ThermoFisher Scientific (Waltham, MA). CleanCap EGFP mRNA was obtained from TriLink Biotechnologies (San Diego, CA).

Polymer synthesis

A block co-polymer of PACE-PEG with a molecular weight of 30.9 kDa was synthesized using enzyme-catalyzed copolymerization as previously described, with some modifications.[12,14] Briefly, PDL was copolymerized with MDEA, DES, and PEG via a CALB enzyme catalyst in diphenyl ether. The reaction proceeded via an initial oligomerization phase at 90°C under 1 atm of argon gas for 24 h, followed by a polymerization phase at 90°C under vacuum for 48 h. After synthesis, diphenyl ether solvent was removed via three hexane washes, and the PACE-PEG polymer was dissolved in chloroform and filtered. The solvent was removed using a rotary evaporator, and the polymer was stored at ≤–20°C until use.

Nanoparticle formulation and characterization

PLGA and PACE-PEG NPs were formulated using a single oil-in-water (o/w) or double water-in-oil-in-water (w/o/w) emulsion solvent evaporation technique. NPs encapsulating lipophilic fluorescent DiD dye were formulated using a single emulsion-solvent evaporation method, as described previously.[12,23] Briefly, 50 mg of polymer was dissolved in 1 mL of dichloromethane or chloroform overnight. For DiD-loaded formulations, 0.5 wt% of dye to polymer was used. Immediately prior to formulation, 25 mL of dye (10 mg/mL in DMSO) was added to the dissolved polymer. This solution was then added dropwise under vortexing into 2 mL of 5 wt% low-molecular-weight PVA solution and sonicated to form an o/w single emulsion. PACE-PEG NPs encapsulating EGFP mRNA were formulated using a double-emulsion evaporation method.[12] Briefly, aqueous nucleic acid cargo was added dropwise under vortexing into the dissolved polymer solution and sonicated using a probe tip sonicator three times for 10 s to form the first water-in-oil emulsion. This emulsion was then added dropwise while vortexing into 2 mL of 5% low molecular weight PVA solution and sonicated to form the w/o/w double emulsion. Both single and double emulsions were then diluted into 10 mL of 0.3% PVA solution while mixing and then transferred to a round-bottom flask. The NP solution was then placed on the rotary evaporator for 15 min to remove the remaining organic solvent. The NPs were washed in pure water by centrifugation. The size and zeta potential of freshly prepared NPs were measured using dynamic light

scattering (Zetasizer Pro, Malvern Panalytical, Malvern, United Kingdom). PLGA NPs were lyophilized, and PACE-PEG NPs were flash frozen in liquid nitrogen and stored at ≤–80°C prior to shipment of materials on dry ice. Prior to NP administration, aliquots were tested for sterility and endotoxin to ensure criteria were met, sonicated, and prepared for administration under sterile conditions.

In vivo studies

All animal procedures conformed to the requirements of the Animal Welfare Act, and protocols were approved prior to implementation by the Institutional Animal Care and Use Committee at the University of California, Davis. Activities related to animal care were performed according to California National Primate Research Center standard operating procedures. Female rhesus monkeys with a prior history of pregnancy were time-mated and identified as pregnant by ultrasound according to established methods.[22] Prior to study assignment, dams were sedated with ketamine (IM, ∼10 mg/kg), and normal fetal growth and development were confirmed by ultrasound. Dams were selected for the study (N = 8; 6–13 years of age, 5.0–9.5 kg; N = 3 fetal PLGA DiD; N = 3 fetal PACE-PEG DiD [75–80 days gestational age; term 165 ± 10 days]; N = 2 fetal PACE-PEG EGFP mRNA [90 days gestational age]) (Table 1) according to established protocols.[22] On the day of fetal NP delivery, dams were sedated with telazol (IM; 5–8 mg/kg), and under sterile conditions as previously described, an ∼300 mL NP volume (30 mg) was carefully injected via the fetal portal vein as it traverses the fetal liver under ultrasound guidance.[22] Normal fetal growth, development, and fetal heart rate and rhythm were confirmed sonographically prior to and post-NP delivery, as well as immediately prior to hysterotomy. Hysterotomies were scheduled for fetal tissue collection 24 (DiD NPs; N = 6) or 48 (EGFP NPs; N = 2) h post-administration for analysis of outcomes. Maternal complete blood counts were assessed immediately prior to surgery (all within normal limits), and dams remained healthy and robust during the study period. All dams were returned to the breeding colony post-hysterotomy.

Table 1. *Summary of Fetal Rhesus Macaque Nanoparticle (NP) Administration*

Fetal identifier	*Polymeric NP administered*	*Gestational age (Sex)*	*Body weight (g)*
A	PLGA DiD	75 days (male)	46.0
B	PLGA DiD	80 days (male)	65.2
C	PLGA DiD	80 days (male)	51.7
D	PACE-PEG DiD	80 days (male)	64.6
E	PACE-PEG DiD	75 days (female)	42.9
F	PACE-PEG DiD	75 days (male)	57.0
G	PACE-PEG EGFP mRNA	90 days (male)	107.3
H	PACE-PEG EGFP mRNA	90 days (male)	99.7

All fetuses were administered 3 mg of polymeric NPs and were assessed within 24 (PLGA and PACE-PEG) or 48 h (PACE-PEG EGFP mRNA) post-administration to evaluate efficiency of transfer and biodistribution.

Fetal tissues were collected according to established protocols.[24,25] The gestational sac was carefully removed intact from the uterus under aseptic conditions (*e.g.,* the gestational sac was manually dissected at the level of decidua, ensuring amniotic fluid, fetus, and placenta remained intact for analysis). All procedures were performed using sterile technique. Amniotic fluid was collected (selected area devoid of placenta and distal to the fetus and umbilical cord), then the gestational sac was opened with the fetus attached to the placenta via the umbilical cord and initially imaged (data not shown) using far-red fluorescence imaging (IVIS® Spectrum, Revvity, Waltham, MA; far-red channel [ex/em 640/680]). Fetal blood and urine were collected and imaged separately. Results confirmed no evidence of fluorescence in these specimens. The umbilical cord was then clamped and cut and removed with the placenta and weighed, then fetal body weights and measures were assessed (all within normal limits). Tissues collected included the brain (right and left cerebral hemispheres, right and left cerebellum); cervical spinal cord; thymus; heart (right and left ventricles); lung lobes (right and left cranial, middle, caudal, and accessory lobes); omentum; spleen; pancreas; liver (quadrate, right, left, and caudate lobes); right and left adrenals; right and left kidneys; right and left gonads; reproductive tract; right and left quadriceps; gastrointestinal (GI) tract (stomach, duodenum, jejunum, ileum, and colon); long bone (femur); skin; umbilical cord; placental disks (primary and secondary disks); membranes (amnion and chorion); and decidua. Tissues were imaged (Fig. 1) then flash frozen over liquid nitrogen in sterile Sarstedt tubes with RNAlater. Tissues were also placed in cassettes with optimal cutting temperature (OCT) embedding compound and quickly frozen over liquid nitrogen (see below). OCT cassettes were shipped to Yale on the day of collection on dry ice for microscopic analysis (cerebral hemispheres, thymus, heart, lung lobes, omentum, spleen, pancreas, liver lobes, adrenal glands, kidneys, gonads, muscle, ileum, colon, bone, skin, and placenta) (Supplementary Fig. S1 and Fig. S2). Sections of select tissues were also placed into histology cassettes and immersed in 10% phosphate-buffered formalin. Cassettes were embedded in paraffin, sectioned at 5–6 μm, mounted on glass slides, then stained with hematoxylin and eosin (H&E) according to standardized protocols (Supplementary Fig. S3). H&E-stained sections were imaged using an Olympus BX51 light microscope (Olympus Corporation, Tokyo, Japan).

OCT-embedded tissues

Frozen sections (10 μm thickness from OCT-embedded tissues) were mounted on glass slides with 4',6-diamidino-2-phenylindole (DAPI) and Hoechst 33342 nuclear counterstain. Images of tissues from the DiD NP-treated fetuses were acquired using an EVOS FL Auto 2 Cell Imaging System with a standard Cy5 filter with an Olympus superapochromat 20x/0.75 NA objective. Images of tissues from the EGFP NP-treated group were acquired using an EVOS M5000 Imaging System. Tissues from fetuses administered PACE-PEG EGFP NPs were used as a control (non-far-red fluorescence) for microscopic analysis (contained no DiD component in the NPs and EGFP emission does not overlap with DiD emission). Similarly, tissues from fetuses administered PACE-PEG DiD NPs were used for microscopic analysis (no EGFP component in the NPs and DiD emission and does not overlap with EGFP emission). All images for all figures were obtained under comparable settings (*e.g.,* exposure time, light intensity) to quantitatively compare across the tissues within each dataset. All images were processed in FIJI software (version 2.1.0) and relative fluorescence was calculated using a custom routine coded with MATLAB, which has been previously described.[13,26,27] Briefly, the background threshold for each channel was set based on non-green or non-far-red fluorescence images, as appropriate. The positive fluorescence intensity values were summed for each treated sample image, and the fluorescence intensity values for images corresponding to each organ were averaged for comparison per fetus. The effects of nuclear signal thresholding based on DAPI/Hoechst 33342 staining is shown in Supplementary Figure S4.

Quantitative PCR

A section of frozen tissues (approximately 30 mg per sample) was thawed in 500 mL of RNAlater Stabilization Solution (ThermoFisher) then washed and rehydrated in PBS. Buffer RLT (Qiagen) with β-mercaptoethanol was added to each sample and was then homogenized for 5 s using an Omni Tissue Homogenizer (Omni), then placed on ice. The samples were then added to a QIAShredder column (Qiagen) and centrifuged for 2 min at 21,000 *g*. RNA was extracted from homogenized tissues using the RNeasy Mini Kit (Qiagen 74106) according to the manufacturer's instructions and eluted in 50 mL of water. The concentration of the extracted RNA samples was measured using a Nanodrop (Thermo Fisher), and 1 μg of RNA was used for conversion to cDNA with the high-capacity cDNA Reverse Transcription Kit (Applied Biosystems). cDNA conversion was set up as follows: 2 mL 10x RT buffer, 0.8 mL 25x dNTP mix, 2 mL 10x random primers, 1 mL MultiScribe RTase, 1 mL RNase inhibitor, 3.2 mL nuclease-free dH_2O. Thermocycler conditions were as follows: 25°C for 10 min, 37°C for 120 min, 85°C for 5 min, then hold at 4°C. cDNA concentrations were measured using a Nanodrop, and the resulting reaction was diluted 1:10 with water. For qPCR, 1 mg of cDNA was aliquoted for analysis in a StepOnePLUS Real-Time PCR System (Applied Biosystems). Reactions were conducted in triplicate for each sample. qPCR was set up as follows: 1.25 mL of TaqMan gene-specific probes (actin and EGFP), 12.5 mL of TaqMan Fast Universal PCR Master Mix (2x), and 6.28 mL of nuclease-free dH_2O. Thermocycler conditions were as follows: 95°C for 20 s, 95°C for 1 s, and 60°C for 20 s x 40 cycles, then hold at 4°C. Expression relative to the tissues exposed to PACE-PEG DiD NPs, which was used as a non-mRNA treated group for comparison, was recorded as fold-change and calculated from average C_T values using the $\Delta\Delta C_T$ method.

Statistical analysis

Results were analyzed using GraphPad Prism (version 10.0.0). Data are presented as individual data points or as mean ± standard deviation (SD) or standard error of the mean as indicated. Where possible, Dunnett's one-way ANOVA with multiple comparisons test or an unpaired *t*-test ($\alpha = 0.05$) was used as appropriate. For all statistical tests, $p \leq 0.05$ was considered statistically significant.

RESULTS

PLGA and PACE-PEG NPs

To evaluate the impact of polymer type on NP biodistribution after fetal rhesus delivery, PLGA and PACE-PEG NPs were formulated encapsulating a DiD fluorescent dye using a single emulsion solvent evaporation formulation method.[12,13] The PLGA DiD NPs, which were ~260 nm in hydrodynamic diameter, were larger than the PACE-PEG NPs, which were ~175 nm in diameter (Table 2). As expected, the PLGA DiD NPs had a negative surface charge of −28 mV, whereas the PACE-PEG DiD NPs had a positive surface charge of +25 mV.

Fetal outcomes post-administration

Fetuses were assessed sonographically immediately prior to hysterotomy and showed normal growth, development, and heart rates. All fetal organs, amniotic fluid

Table 2. *Characterization Data for DiD and EGFP mRNA PLGA and PACE-PEG NP Formulations*

Material and cargo	*Diameter (nm)*	*Polydispersity index (PDI)*	*Zeta potential (mV)*
PLGA (0.5 wt% DiD)	261 ± 4	0.15	−28.4 ± 1.1
PACE-PEG (0.5 wt% DiD)	175 ± 3	0.20	25.0 ± 0.8
PACE-PEG (EGFP mRNA)	147 ± 2	0.18	21.4 ± 0.3

volumes, and the placenta were within normal limits, which was confirmed grossly when tissues were evaluated. Select fetal tissues were compared to historical control fetuses of comparable gestational ages (H&E staining). No abnormal findings were observed, and no differences were identified when compared to control fetuses (Supplementary Fig. S3). Thus, this short-term study did not indicate any adverse events.

Biodistribution

To assess NP biodistribution, fetal tissues were collected 24 h post-DiD NP administration as described above. PLGA DiD NPs ($N = 3$) showed accumulation primarily in the fetal liver and spleen, with minimal but detectable distribution to the GI tract and kidneys (Fig. 1). The PACE-PEG DiD NPs ($N = 3$) exhibited more widespread biodistribution compared to PLGA. In addition to the liver and spleen, PACE-PEG NPs were also found in the lung lobes, GI tract, and kidneys. The omentum demonstrated significant expression of both NPs.

Quantitative fluorescence microscopic analysis of fetal tissues was accomplished using a custom MATLAB

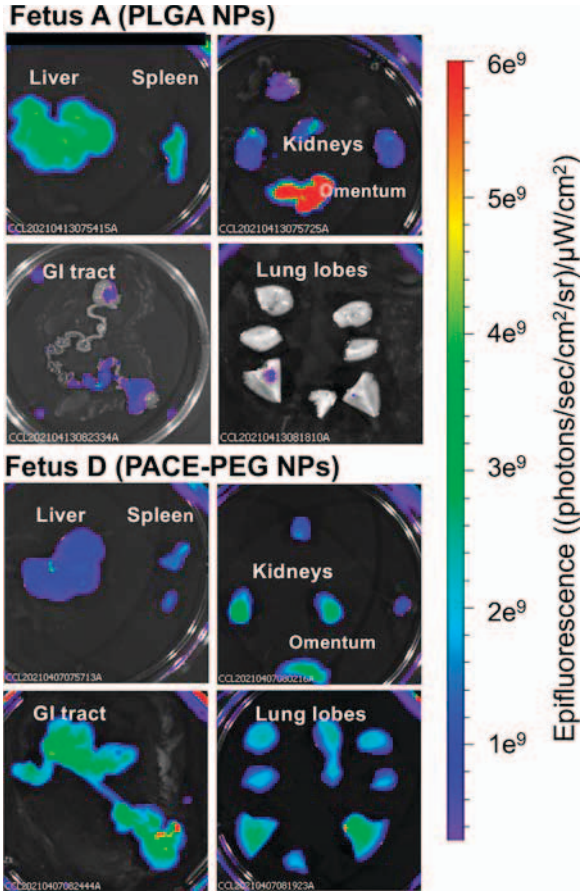

Figure 1. Whole tissue fluorescence imaging. Biodistribution of polymeric NPs after fetal delivery in early gestation. Fetal tissues were collected 24 h after PLGA NP (Fetus A) or PAGE-PEG DiD NP (Fetus D) portal vein administration under ultrasound guidance.

code[13,26,27] (Supplementary Fig. S1). Consistent with the IVIS Spectrum far-red fluorescence imaging results, the highest fluorescent signal for PLGA DiD NP-administered fetuses was the spleen, omentum, and liver (Fig. 2). The next highest fluorescence signal was found in the adrenal glands, which was approximately two orders of magnitude lower than the signal detected in the spleen. Of note, no measurable fluorescence signal from NPs was found in the placenta in all fetuses assessed (not shown). In the pooled analysis, each data set represents the average of imaged tissue sections from three fetuses in each of the groups (Table 1). To examine consistency across the measurements from each individual tissue, the quantified fluorescence intensity was also plotted separately for each fetus. To quantify the extent of biodistribution to extrahepatic tissues, an organ metric was utilized: the number of extrahepatic tissues that demonstrated statistically significant NP uptake, defined as tissues where all representative images showed evidence of fluorescence signal significantly above background in all three fetuses. For the PLGA NPs, the metric was 8, 6, and 6 in the three fetuses evaluated. In addition to the liver, there was significant fluorescence noted in the spleen, omentum, and pancreas.

Comparable analysis was performed on tissues from the fetuses that received PACE-PEG NPs. Quantitative microscopic analysis of tissues revealed that the highest level of fluorescence signal was found in the omentum, spleen, and heart (Fig. 3). The 10 tissues with the highest signals in the PACE-PEG group had consistent findings in intensity across the group, as all were within one order of magnitude of the highest fluorescence signal. The placenta in the PACE-PEG group also showed no fluorescence signal (not shown).

Since the tissue fluorescence found with PACE-PEG DiD NPs was generally lower in intensity than the fluorescence in fetuses administered PLGA NPs, which may have been due to a lower level of DiD loading in the PACE-PEG NPs compared to PLGA NPs, a higher exposure time and gain were used to acquire images for the PACE-PEG dataset. Due to this discrepancy in raw signal intensity between the PLGA and PACE-PEG NPs, the fluorescence signal was normalized in each tissue to the liver fluorescence signal to compare the relative amount of accumulation in fetal tissues across the two NP types. In the PLGA NP-treated group, the spleen and omentum exhibited approximately 20 times and 10 times the signal intensity of the liver, respectively (Fig. 2) (Supplementary Fig. S4). All other tissues had negligible signal intensity when compared to the liver. In the PACE-PEG NP group, the omentum showed approximately 4 times the signal intensity of the liver. The spleen, heart, and kidneys

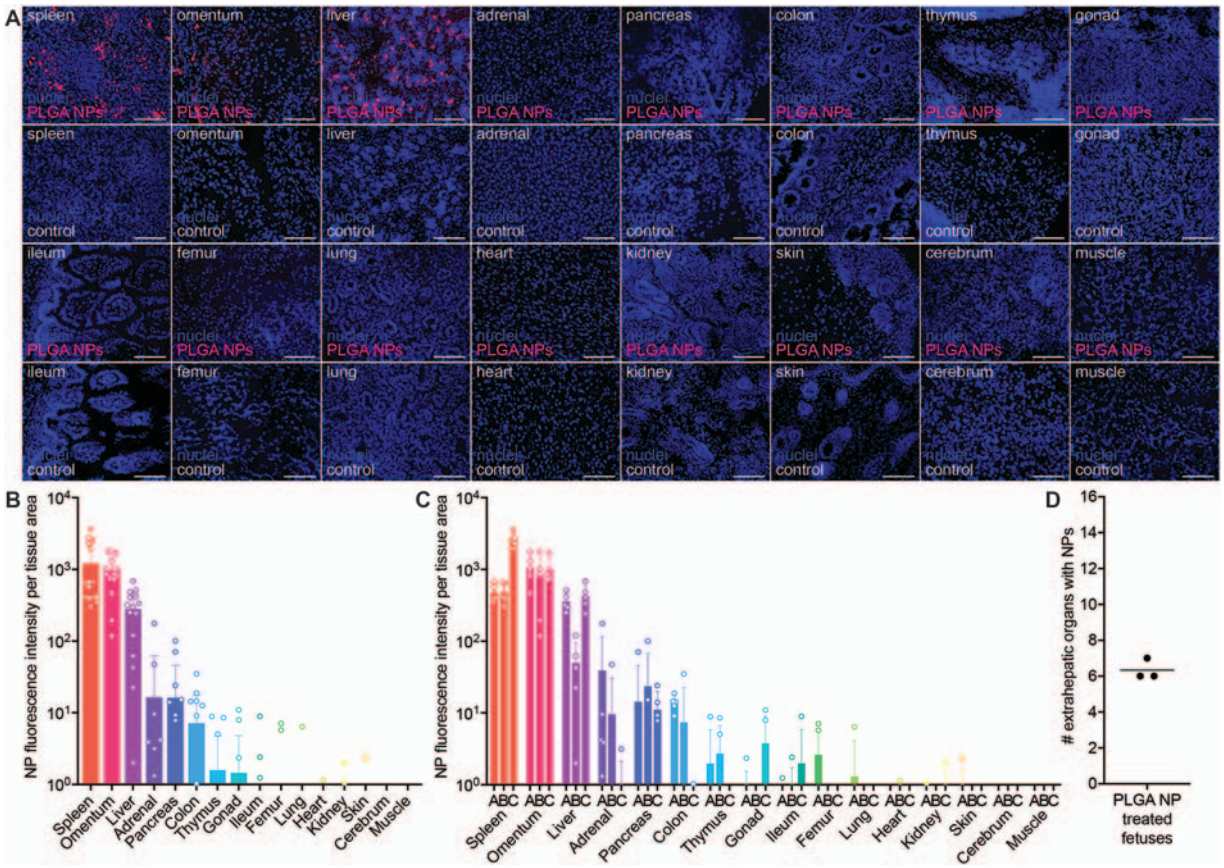

Figure 2. Fluorescence microscopy: Biodistribution of PLGA NPs. **(A)** Representative fluorescence images from Fetus A (*top*) administered PLGA DiD NPs and Fetus G (bottom) without the red fluorescent label ranked by highest relative DiD fluorescence observed. Blue = DAPI, Red = DiD, 20X magnification, scale bar = 100 mm. **(B)** Comparison of fluorescence intensity from fetal tissues averaged from five representative images each for three fetuses (Fetuses A, B, C) and ranked by highest relative fluorescence intensity observed. **(C)** Comparison of fluorescence intensity from individual fetuses for tissues with fluorescence signal above background. **(D)** Number of extrahepatic tissues that demonstrated NP uptake, defined as tissues where all five representative images exhibited fluorescence signal above background (Fetuses A, B, C). Each point represents an individual fetus ($N = 3$).

showed 1–2 times signal intensity of the liver. All other organs with measurable signal had less than 1 time the signal intensity of the liver. Applying this metric for biodistribution beyond the liver to the PACE-PEG NPs, the extrahepatic organ metric was 12, 13, and 14 in the three fetuses evaluated, further confirming that PACE-PEG NPs exhibit more widespread biodistribution.

Functional reporter mRNA expression

Since the PACE-PEG polymer is mildly cationic, efficient at encapsulation of negatively charged nucleic acids, and exhibits the most widespread NP biodistribution, this class of NP was used for fetal mRNA delivery. PACE-PEG NPs were formulated encapsulating EGFP mRNA.[11,12,14] The PACE-PEG EGFP mRNA NPs, formulated via a double emulsion solvent evaporation method,[12,13] had similar characteristics to PACE-PEG DiD NPs, with a diameter of ~150 nm and a positive surface charge of +21 mV (Table 2). Tissues were collected 48 h post-administration to assess protein expression. Fetuses administered PACE-PEG DiD NPs were included as a non-green fluorescence test group for comparison and to address any potential impact related to the presence of the PACE-PEG polymer (Fig. 4). Several tissues demonstrated positive EGFP expression, which was defined as a measurable green fluorescence signal above the level of background in tissues from fetuses without EGFP. Quantitative analysis of the microscopy images revealed that the highest green fluorescence signal was found in the fetal liver. To corroborate these findings with EGFP expression, RNA was extracted and converted to cDNA for analysis by qPCR. EGFP mRNA was detected in select tissues (*e.g.,* liver, spleen, kidneys, adrenal glands, quadriceps, ileum, skin) in the two fetuses analyzed (Fig. 4).

DISCUSSION

In this preliminary study, we have demonstrated that polymeric NPs are a potential platform for nonviral delivery of nucleic acid therapeutics under the conditions

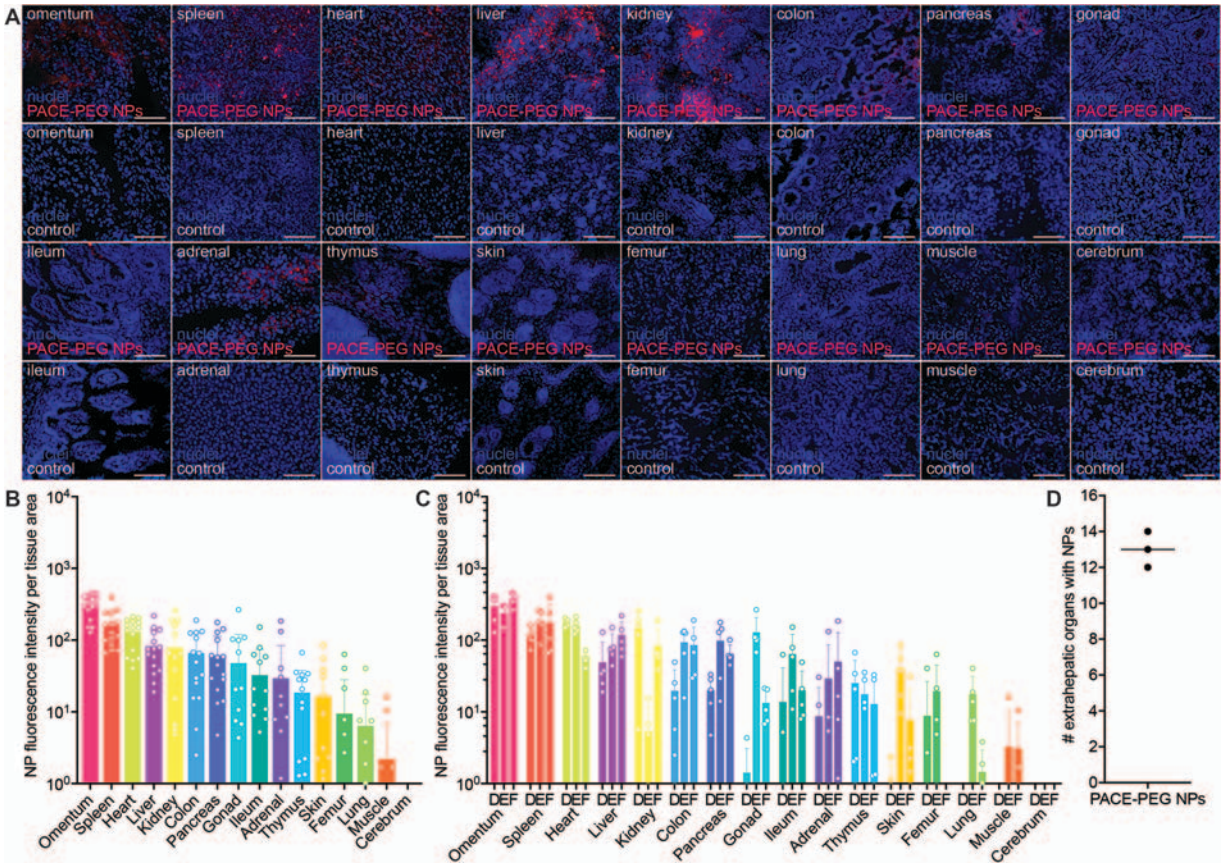

Figure 3. Fluorescence microscopy: Biodistribution of PACE-PEG NPs. **(A)** Representative images of fetal tissues from Fetus D (*top*) administered PACE-PEG DiD NPs and Fetus G (*bottom*) without a red fluorescent label ranked by highest relative DiD fluorescence observed. Blue = DAPI, Red = DiD, 20X magnification, scale bar = 100 mm. **(B)** Comparison of fluorescence intensity from fetal tissues averaged from five representative images each for Fetuses D and F (males) and Fetus E (female) and ranked by highest relative fluorescence intensity observed. **(C)** Comparison of fluorescence of individual fetuses for tissues with fluorescence signal above background. **(D)** Number of extrahepatic tissues that demonstrated NP uptake, defined as tissues for which all five representative images displayed fluorescence signal above background (Fetus D, E, F). Each point represents an individual fetus ($N = 3$).

described. These investigations indicated that NPs formed from PLGA, which is a material found in many FDA-approved products, accumulate in the fetal liver and spleen after administration via the portal vein. In adult mice, the hydrodynamic diameter of PLGA NPs is known to have a significant effect on biodistribution; NPs with diameters similar to those used in the study described here were preferentially sequestered in the mouse liver and spleen after intravenous administration.[28] While short-term safety has been shown, further studies are required to assess the long-term ramifications as well as the specific cell populations that can be targeted by PACE-PEG NPs. Moreover, alterations in polymer chemistry[12,13,29] and conjugation of targeting moieties[13,26] offer additional avenues for the optimization of PACE-PEG, which will be crucial for targeting tissues as they relate to specific diseases where such treatments could be curative. Considerations include the differences in behavior of PLGA NPs and PACE-PEG NPs, including chemical properties, size, and surface charge. Smaller NPs generally exhibit more widespread biodistribution, and PEGylated NPs show greater stability and extended circulation time,[13,28] which under some circumstances might be beneficial. *In vitro* cell culture studies using multiple cell lines comparing PLGA NPs to PACE-PEG NPs suggest that PACE-PEG NPs exhibit higher uptake but comparable biocompatibility compared to PLGA NPs, likely due to their mildly cationic charge.[12,29]

The study described here also tested the potential of PACE-PEG as an alternative class of polymeric NPs to consider for potential therapeutic applications. PACE-PEG is a polymer that offers high nucleic acid encapsulation efficiency and a wide biodistribution profile.[11,12,14] PEGylation is known to improve the circulation time of NPs after systemic administration and shield NPs from early phagocytic clearance by lending a stealth profile as noted.[15–17] Both properties may play a role in the more widespread biodistribution demonstrated by PACE-PEG NPs in this short-term study. While PACE-PEG NPs reached multiple fetal tissues (*e.g.,* heart, lungs, kidneys, pancreas, GI tract), a more selective approach is likely advantageous. Further studies are needed to assess the

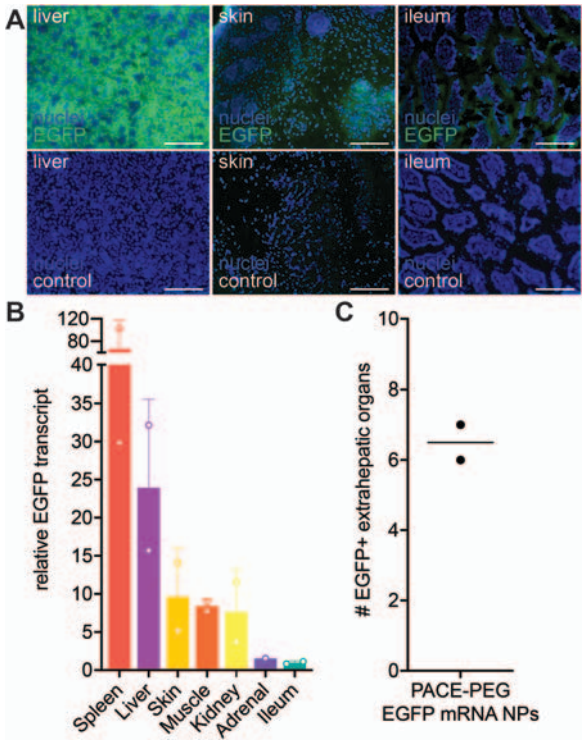

Figure 4. EGFP reporter gene expression. **(A)** (*top*) Representative images of tissues with high (liver), mid-level (skin), and low (ileum) EGFP expression from Fetuses G, H, and G, respectively, administered PACE-PEG EGFP mRNA NPs and (*bottom*) compared to a fetus with no fluorescent reporter mRNA administered. Blue = DAPI, Green = EGFP, 20X magnification, scale bars = 100 mm. **(B)** Relative EGFP transcript levels in fetal tissues from Fetuses G and H administered PACE-PEG EGFP mRNA NPs. **(C)** Total number of tissues identified as EGFP mRNA positive by qPCR. Each point represents an individual fetus ($N = 2$).

specific cell populations that can be targeted by PACE-PEG NPs through this strategy. Moreover, alterations in polymer chemistry[12,13,30] and conjugation of targeting moieties[13,26] as we have previously reported, may offer additional avenues for the optimization of PACE-PEG for specific inherited diseases that involve individual or multiple organ systems.

However, as has been demonstrated in humans and nonhuman primates, prior exposure to a range of products that are PEGylated can induce anti-PEG antibodies, and hypersensitivity reactions have been reported in human clinical trials.[18] While prenatal transfer typically avoids immune responses in the developing embryo and early gestation fetus, NPs that include PEG require screening the dams prior to study assignment and fetal administration.

Of note, NP biodistribution is not a guarantee of downstream success of cellular gene correction or gene addition. Endosomal escape and internalization of mRNA cargo are also key to functional outcomes.[11,31–33] The intent of this short-term study was to address immediate findings after administration as a first step in assessing the overall features when comparing PLGA to PACE-PEG NPs. Further studies will be needed to pursue long-term outcomes and safety as well as efficiency for organ-targeting, including the potential for germ cell gene transfer, and at the level of detail required. Our previous studies have focused on this question in fetal rhesus macaques administered lentiviral vectors in early gestation (late first trimester) using systemic or organ targeting approaches.[34] In these studies, laser capture microdissection was used to isolate germ cells, surrounding stroma, and the surface epithelium for qPCR. No sequences were detected in genomic DNA isolated from spermatogonia, and very low copies were detected in surrounding stromal cells obtained from both male and female gonads (*e.g.,* near-term fetuses and postnatal ~3 months of age). Organ-targeted approaches (*e.g.,* heart, lung) have consistently shown no evidence of germ cell gene transfer. For systemic administration (*e.g.,* fetal intraperitoneal), there was no indication of germ cell gene transfer in males, whereas a subset of female fetuses showed PCR-positive oocytes. As noted in this publication, timing is likely critical based on developmental events at the time of transfer (late first trimester).[34] Similar studies will be required to address these and related questions, including any potential immune responses, when considering applications of PLGA and PACE-PEG NPs and the optimal methods for use. As is the case when considering any viral or nonviral vector, the combination of vector design and route of administration are both crucial to ensuring safety as well as targeting essential populations *in vivo* relevant to the disease(s) of interest.[24,25,34–36] While these studies focused on short-term outcomes after prenatal administration, safety was shown under these conditions, as all fetuses remained viable with no evidence of adverse events during this sensitive period of development.

CONCLUSIONS

This preliminary proof-of-concept study represents an initial assessment comparing polymeric NPs in the fetal rhesus monkey with short-term analysis of biodistribution and safety. While PLGA NPs demonstrated targeting primarily to the fetal liver and spleen, PACE-PEG NPs resulted in more widespread biodistribution. This preliminary study provides evidence to support further detailed assessments with long-term analysis that focuses on safety and efficiency. Polymeric NPs are promising candidates for delivery of therapeutic gene cargoes and may require a head-to-head comparison with other common delivery vehicles for targeting specific cells and tissues, including a range of AAV serotypes.

ACKNOWLEDGMENTS

This study was supported by a NIH Somatic Cell Genome Editing (SCGE) Consortium Collaborative Opportunity Fund award to Yale University (UG3/UH3-

HL147352) and the Nonhuman Primate Testing Center for Evaluation of Somatic Cell Genome Editing Tools at UC Davis (U42-OD027094, AFT). Information about these studies is also provided in the SCGE Toolkit, supported through the SCGE Dissemination and Coordinating Center, which is a platform housing data generated across all Consortium initiatives.[37]

AUTHORS' CONTRIBUTIONS

A.S.P.-D.—Conceptualization, funding acquisition, methodology, investigation, data curation, formal analysis, writing—original draft, writing—review and editing; A.Y.L.—Methodology, investigation, data curation, formal analysis, writing—original draft, writing—review and editing; D.A.E.—Investigation, formal analysis, writing—review and editing; L.G.B.—Formal analysis, writing—review and editing; A.I.M.—Formal analysis, writing—review and editing; R.D.M.—Investigation; D.H.S.—Formal analysis, writing—review and editing; M.L.M.—Investigation, formal analysis, writing—review and editing; C.C.L.—Investigation, formal analysis, writing—review and editing; H.J.K.—Formal analysis, writing—review and editing; P.M.G.—Conceptualization, funding acquisition, methodology, supervision, writing—review and editing; A.F.T.—Conceptualization, funding acquisition, methodology, investigation, formal analysis, supervision, writing—original draft, writing—review and editing; W.M.S.—Conceptualization, funding acquisition, methodology, supervision, writing—review and editing.

AUTHOR DISCLOSURE STATEMENT

W.M.S. is a co-founder of Stradefy Biosciences, Xanadu Bio, and B3 Therapeutics. W.M.S. is a consultant to Xanadu Bio, B3 Therapeutics, Stradefy Biosciences, Johnson & Johnson, Celanese, Cranius, and CMC Pharma. A.S.P. is a co-founder and former consultant of Xanadu Bio. D.A.E. is a consultant to Xanadu Bio. W.M.S., L.G.B., P.M.G., and A.S.P. are listed as inventors on patent applications relating to PACE delivery of nucleic acids. A.S.P., W.M.S., D.H.S., and P.M.G. are inventors on patents and patent applications involving polymer nanoparticles for *in utero* gene editing and drug delivery. W.M.S. had a sponsored research project with Xanadu Bio. The other authors declare that they have no competing interests.

FUNDING INFORMATION

This study was supported by a Collaborative Opportunity Fund award provided through the NIH SCGE Consortium as noted above (UG3-HL147352, WMS and PMG; U42-OD027094, AFT), and NIH grants R01-HL125892 (PMG, WMS), U01-AI145965 (PMG, WMS), and P51-OD011107 (Primate Center base operating grant, AFT). *In vivo* imaging was performed with instrumentation obtained through NIH S10 High-End Instrumentation grants (S10-OD016261 and S10-OD018012; AFT). ASP was supported by a Postdoc-to-Faculty Transition Award from the Cystic Fibrosis Foundation (PIOTRO21F5) and a K99/R00 Pathway to Independence Award from the NIH (K99/R00-HL151806). AYL was supported by an NIH F30 Individual Predoctoral Fellowship (F30-HD106692) and a T32 training grant (T32-GM13665). LGB was supported by a K99/R00 Pathway to Independence Award from the NIH (K99/R00-HL157552).

SUPPLEMENTARY MATERIAL

Supplementary Figures

REFERENCES

1. Bahal R, Ali McNeer N, Quijano E, et al. *In vivo* correction of anaemia in β-thalassemic mice by γPNA-mediated gene editing with nanoparticle delivery. Nat Commun 2016;7:13304; doi: 10.1038/ncomms13304

2. Cun D, Foged C, Yang M, et al. Preparation and characterization of poly(DL-lactide-co-glycolide) nanoparticles for siRNA delivery. Int J Pharm 2010;390(1):70–75; doi: 10.1016/j.ijpharm.2009.10.023

3. Fields RJ, Quijano E, McNeer NA, et al. Modified poly(lactic-co-glycolic acid) nanoparticles for enhanced cellular uptake and gene editing in the lung. Adv Healthc Mater 2015;4(3):361–366; doi: 10.1002/adhm.201400355

4. McNeer NA, Chin JY, Schleifman EB, et al. Nanoparticles deliver triplex-forming PNAs for site-specific genomic recombination in CD34+ human hematopoietic progenitors. Mol Ther 2011;19(1):172–180; doi: 10.1038/mt.2010.200

5. Piotrowski-Daspit AS, Barone C, Lin CY, et al. *In vivo* correction of cystic fibrosis mediated by PNA nanoparticles. Sci Adv 2022;8(40):eabo0522; doi: 10.1126/sciadv.abo0522

6. Luo D, Woodrow-Mumford K, Belcheva N, et al. Controlled DNA delivery systems. Pharm Res 1999;16(8):1300–1308; doi: 10.1023/a:1014870102295

7. Lv H, Zhang S, Wang B, et al. Toxicity of cationic lipids and cationic polymers in gene delivery. J Control Release 2006;114(1):100–109; doi: 10.1016/j.jconrel.2006.04.014

8. Monnery BD, Wright M, Cavill R, et al. Cytotoxicity of polycations: Relationship of molecular weight and the hydrolytic theory of the

mechanism of toxicity. Int J Pharm 2017;521(1–2):249–258; doi: 10.1016/j.ijpharm.2017.02.048

9. Pack DW, Hoffman AS, Pun S, et al. Design and development of polymers for gene delivery. Nat Rev Drug Discov 2005;4(7):581–593; doi: 10.1038/nrd1775

10. Cui J, Piotrowski-Daspit AS, Zhang J, et al. Poly (amine-co-ester) nanoparticles for effective Nogo-B knockdown in the liver. J Control Release 2019;304:259–267; doi: 10.1016/j.jconrel.2019.04.044

11. Jiang Y, Lu Q, Wang Y, et al. Quantitating endosomal escape of a library of polymers for mRNA delivery. Nano Lett 2020;20(2):1117–1123; doi: 10.1021/acs.nanolett.9b04426

12. Kauffman AC, Piotrowski-Daspit AS, Nakazawa KH, et al. Tunability of biodegradable Poly (amine-co-ester) polymers for customized nucleic acid delivery and other biomedical applications. Biomacromolecules 2018;19(9):3861–3873; doi: 10.1021/acs.biomac.8b00997

13. Piotrowski-Daspit AS, Bracaglia LG, Eaton DA, et al. Enhancing *in vivo* cell and tissue targeting by modulation of polymer nanoparticles and macrophage decoys. Nat Commun 2024;15(1):4247; doi: 10.1038/s41467-024-48442-7

14. Zhou J, Liu J, Cheng CJ, et al. Biodegradable Poly(amine-co-ester) terpolymers for targeted gene delivery. Nat Mater 2011;11(1):82–90; doi: 10.1038/nmat3187

15. Harris JM, Chess RB. Effect of pegylation on pharmaceuticals. Nat Rev Drug Discov 2003;2(3):214–221; doi: 10.1038/nrd1033

16. Piotrowski-Daspit AS, Kauffman AC, Bracaglia LG, et al. Polymeric vehicles for nucleic acid delivery. Adv Drug Deliv Rev 2020;156:119–132; doi: 10.1016/j.addr.2020.06.014

17. Shi L, Zhang J, Zhao M, et al. Effects of polyethylene glycol on the surface of nanoparticles for targeted drug delivery. Nanoscale 2021;13(24):10748–10764; doi: 10.1039/d1nr02065j

18. Moreno A, Pitoc GA, Ganson NJ, et al. Anti-PEG antibodies inhibit the anticoagulant activity of PEGylated aptamers. Cell Chem Biol 2019;26(5):634–644.e3; doi: 10.1016/j.chembiol.2019.02.001

19. Grun MK, Suberi A, Shin K, et al. PEGylation of poly(amine-co-ester) polyplexes for tunable gene delivery. Biomaterials 2021;272:120780; doi: 10.1016/j.biomaterials.2021.120780

20. Cullis PR, Felgner PR. The 60-year evolution of lipid nanoparticles for nucleic acid delivery. Nat Rev Drug Discov 2024;23(9):709–722; doi: 10.1038/s41573-024-00977-6

21. Tarantal AF, Noctor SC, Hartigan-O'Connor DJ. Nonhuman primates in translational research. Annu Rev Anim Biosci 2022;10:441–468; doi: 10.1146/annurev-animal-021419-083813

22. Tarantal AF. Chapter 20: Ultrasound imaging in rhesus (*Macaca mulatta*) and long-tailed (*Macaca fascicularis*) macaques: Reproductive and research applications. In: The Laboratory Primate. (Woolf-Coote, S., eds.) Elsevier; 2005; pp. 317–351.

23. Park JK, Utsumi T, Seo YE, et al. Cellular distribution of injected PLGA-nanoparticles in the liver. Nanomedicine 2016;12(5):1365–1374; doi: 10.1016/j.nano.2016.01.013

24. Jimenez DF, Lee CI, O'Shea CE, et al. HIV-1-derived lentiviral vectors and fetal route of administration on transgene biodistribution and expression in rhesus monkeys. Gene Ther 2005;12(10):821–830; doi: 10.1038/sj.gt.3302464

25. Tarantal AF, McDonald RJ, Jimenez DF, et al. Intrapulmonary and intramyocardial gene transfer in rhesus monkeys: Safety and efficiency of lentiviral vectors for fetal gene delivery. Mol Ther 2005;12(1):87–98; doi: 10.1016/j.ymthe.2005.01.019

26. Albert C, Bracaglia L, Koide A, et al. Monobody adapter for functional antibody display on nanoparticles for adaptable targeted delivery applications. Nat Commun 2022;13(1):5998; doi: 10.1038/s41467-022-33490-8

27. Bracaglia LG, Piotrowski-Daspit AS, Lin CY, et al. High-throughput quantitative microscopy-based half-life measurements of intravenously injected agents. Proc Natl Acad Sci U S A 2020;117(7):3502–3508; doi: 10.1073/pnas.1915450117

28. Mandl HK, Quijano E, Suh HW, et al. Optimizing biodegradable nanoparticle size for tissue-specific delivery. J Control Release 2019;314:92–101; doi: 10.1016/j.jconrel.2019.09.020

29. Misslick KA, Baldeschwieler JD. Evidence for the role of proteoglycans in cation-mediated gene transfer. Proc Natl Acad Sci USA 1996;93(22):12349–12354; doi: 10.1073/pnas.93.22.12349

30. Jiang Y, Gaudin A, Zhang J, et al. A "top-down" approach to actuate poly(amine-co-ester) terpolymers for potent and safe mRNA delivery. Biomaterials 2018;176:122–130; doi: 10.1016/j.biomaterials.2018.05.043

31. Degors IMS, Wang C, Rehman ZU, et al. Carriers break barriers in drug delivery: Endocytosis and endosomal escape of gene delivery vectors. Acc Chem Res 2019;52(7):1750–1760; doi: 10.1021/acs.accounts.9b00177

32. Namvar A, Bolhassani A, Khairkhah N, et al. Physicochemical properties of polymers: An important system to overcome the cell barriers in gene transfection. Biopolymers 2015;103(7):363–375; doi: 10.1002/bip.22638

33. Xu E, Saltzman WM, Piotrowski-Daspit AS. Escaping the endosome: Assessing cellular trafficking mechanisms of non-viral vehicles. J Control Release 2021;335:465–480; doi: 10.1016/j.jconrel.2021.05.038

34. Lee CC, Jimenez DF, Kohn DB, et al. Fetal gene transfer using lentiviral vectors and the potential for germ cell transduction in rhesus monkeys (*Macaca mulatta*). Hum Gene Ther 2005;16(4):417–425; doi: 10.1089/hum.2005.16.417

35. Tarantal AF, Skarlatos SI. Center for Fetal Monkey Gene Transfer for Heart, Lung, and Blood Diseases: An NHLBI resource for the gene therapy community. Hum Gene Ther 2012;23(11):1130–1135; doi: 10.1089/hum.2012.178

36. Tarantal AF, Lee CC. Long-term luciferase expression monitored by bioluminescence imaging after adeno-associated virus-mediated fetal gene delivery in rhesus monkeys (*Macaca mulatta*). Hum Gene Ther 2010;21(2):143–148; doi: 10.1089/hum.2009.126

37. Saha K, Sontheimer EJ, Brooks PJ, et al.; SCGE Consortium. The NIH somatic cell genome editing consortium. Nature 2021;592(7853):195–204; doi: 10.1038/s41586-021-03191-1

Received for publication October 19, 2025;
accepted after revision December 21, 2025.

Published online: January 22, 2026.